

Effects of Dust in Distorted, Irradiated, and Expanding Atmospheres of Close Binary Components

Mynampati SRINIVASA RAO
Indian Institute of Astrophysics, Bangalore 560034, India
msrao@iiap.ernet.in

(Received 2003 August 22; accepted 2003 October 14)

Abstract

We studied the transfer of line radiation with dust in distorted and expanding atmospheres of close binary components. We assumed that the distortion of the atmosphere is caused by self rotation and a tidal force exerted by the presence of a secondary component. A seventh degree equation is defined to describe the distorted surface for uniform rotation. The equation of line transfer in the presence of gas and dust is solved in the comoving frame of the expanding atmosphere of the primary component in a binary system. We have considered a complete redistribution of photons in the line and that dust scatters radiation isotropically. We used a linear law of velocity of expansion so that the density varies as r^{-3} , where r is the radius of the star, satisfying the law of conservation of mass. We noticed that considerable changes occur in line fluxes in dusty and dust-free atmospheres. The expansion of the atmosphere produces double-peak emission lines with P Cygni characteristics. These emission peaks are reduced in a dusty atmosphere.

Key words: dust — radiative transfer — stars: binaries: close

1. Introduction

A star in a very close binary system has a non-spherical shape because of a rotational distortion and gravitational attraction of the companion of the star. Normal stars are very centrally condensed (Stothers 1974, 1979) and close binaries are usually tidally locked in circular orbits (Giuricin et al. 1984). The shape of the star in a such system can be determined by noting that the potential energy must be the same for each point on star's surface; otherwise, the material would flow down and change the shape of the star.

In general reflection effect is important in a close binary system: usually irradiation can enhance the mass transfer and more irradiation can give rise to even greater mass transfer (Ritter et al. 2000), and thus it is always important to consider a proper irradiation geometry. The spectrum of a supergiant star shows a strong He I absorption line (Ferraro et al. 2003). Thus, based on the effect of irradiation on companions of an accreting neutron star in low-mass X-ray binaries or more on the companions for the strong millisecond pulsars case, one can develop models to simulate this irradiation in the stellar atmosphere. By incorporating a heating effect one may be able to predict the colors of low-mass stars irradiated by a pulsar.

The cases of line transfer in the dusty atmospheres of close binary components that are distorted by self rotation and the tidal effect due to the presence of the companion together with the reflection of light incident from the companion remain practically unexplored. In recent years its importance has been recognized. As is well known, dust grains, such as graphites and silicates, are strongly influenced by radiation, since the cross-section per mass is large.

Recent theoretical studies of close binaries by Peraiah and Srinivasa Rao (1998, hereafter Paper I) have treated the line-transfer problem with a reflection effect in an expanding

atmosphere, while Srinivasa Rao and Peraiah (2000, hereafter Paper II) considered a dusty, expanding atmosphere. In Papers I and II they assumed that stars are spherical in a binary system. In Paper II they found that the scattering of dust increases the core emission. Peraiah and Srinivasa Rao (2002, hereafter Paper III) studied the distorted atmosphere. The distortion is measured by the self rotation and the tidal effect due to the presence of the secondary together with the reflection of the incident radiation on the distorted surface from the secondary, considered to be a point source. The radiation field in the distorted atmosphere consists of two parts: (1) incident radiation from the secondary component and (2) self-radiation of the primary component. The first part, namely the reflected radiation, is calculated by using a one-dimensional rod model (Sobolev 1963), and the second part is treated by using the solution of the transfer equation in spherical symmetry. The contribution of these two radiation fields is used to study the lines formed in the distorted atmosphere. It has been obtained that the absorption features produced due to self radiation vanish and the emission profiles appear when the atmosphere is irradiated. In the next step we would like to apply this method to Iota Orionis, a highly eccentric nearby binary to predict the possible photospheric absorption line profile variability expected to arise due to deformations of the stellar photospheres that results from a tidally driven surface.

The present paper deals with dusty and dust-free atmospheres in a close binary system. It is arranged in the following way. Section 2 describes the calculation of irradiation on the primary from the secondary component, which is a point source, and the method for obtaining a solution of the radiative transfer equation in spherically symmetric atmospheres for calculating the self radiation of the primary star in the presence of dust. Section 3 gives a brief description of the computational procedure, and section 4

is arranged for results and discussions. Finally, section 5 includes conclusions.

2. Basic Equations

2.1. Calculation of Irradiation (S_r) from the Secondary on the Primary Component

We compute the distorted surface by solving a seventh-degree equation derived by Peraiah (1970), and subsequently used in Paper III for solving various values of θ and ϕ , where θ and ϕ are the colatitude and the azimuthal angles, respectively, to obtain the surface for the given parameters: X , f , m_2/m_1 , and r_e/R . Here, X is the ratio of the angular velocities at the equator and pole, f is the ratio of the centrifugal to gravity forces at the equator, m_2/m_1 is the mass ratio of the two components, and r_e/R is the ratio of the radius at the equator to the separation between the centres of gravity of the two components. We always set $X = 1$ for uniform rotation. A numerical solution is obtained with a starting value of $r/r_p = 1$; for details see Peraiah (1969, 1970). We have drawn a schematic diagram in figure 1 for the purpose of computing the ray lengths and for calculating irradiation S_r ; for details refer to Paper III.

Now, we need to estimate the source function due to the self-radiation of the component. This can be done by solving the line-transfer equation for a non-LTE two-level atom in the comoving frame in spherical symmetry.

2.2. Calculation of the Self-Radiation (S_s) of the Primary Component

The spectral lines formed in stellar atmospheres contain information regarding the temperature, pressure, composition, and dynamical state of the gas. Therefore, it is necessary to study the formation of lines in stellar atmospheres. There are several important steps that one has to consider when calculating these lines. These are as follows:

- The effects of the curvature on the radiation field;
- The geometrical extension of the atmospheres;
- Consideration of whether the lines are formed in LTE or in non-LTE;
- Consideration of the photon redistribution regarding whether the line is formed with a complete redistribution or with a partial redistribution;
- The hydrodynamic status of the medium, concerning whether it is expanding, contracting, or static;
- The distribution of the temperature in the atmosphere;
- The effect of the radiation field on the ionization structure of the gas and dust;
- The abundance of the line-forming ions, and this ratio with respect to the abundances of other elements;
- The statistical equilibrium equation representing several levels of the atom;
- The equation of state of the gas of the atmosphere in which we study the pressure, temperature, and composition of the medium.

All of the above characteristics must be taken into account simultaneously to study the spectral line. It is, however, very difficult to include all of these effects into the calculations of the lines simultaneously. We now discuss the comoving frame

calculations while assuming an envelope containing a mixture of gas and dust that is expanding radially.

The equation of line transfer in the comoving frame with absorption and emission due to dust and gas in spherical symmetry (Peraiah, Wehrse 1978; Wehrse, Kalkofen 1985) is given by

$$\begin{aligned} & \mu \frac{\partial I(x, \mu, r)}{\partial r} + \frac{(1 - \mu^2)}{r} \frac{\partial I(x, \mu, r)}{\partial \mu} \\ & = K_L(r)[(\phi(x) + \beta)][S(r, \mu, x) - I(r, \mu, x)] \\ & + \left[(1 - \mu^2) \frac{V(r)}{r} + \mu^2 \frac{dV(r)}{dr} \right] \frac{\partial I(r, \mu, x)}{\partial x} \\ & + K_{\text{dust}} [S_{\text{dust}}(r, \mu, x) - I(r, \mu, x)] \end{aligned} \tag{1}$$

and

$$\begin{aligned} & - \mu \frac{\partial I(x, -\mu, r)}{\partial r} - \frac{(1 - \mu^2)}{r} \frac{\partial I(x, -\mu, r)}{\partial \mu} \\ & = K_L(r)[(\phi(x) + \beta)][S(r, -\mu, x) - I(r, -\mu, x)] \\ & + \left[(1 - \mu^2) \frac{V(r)}{r} + \mu^2 \frac{dV(r)}{dr} \right] \frac{\partial I(r, -\mu, x)}{\partial x} \\ & + K_{\text{dust}} [S_{\text{dust}}(r, -\mu, x) - I(r, -\mu, x)], \end{aligned} \tag{2}$$

where $I(x, \pm\mu, r)$ is the specific intensity of rays at an angle $\cos^{-1} \mu$ [$\mu \in (0, 1)$] with the radius vector at the radial point r with frequency $x [= (v - v_0)/\Delta v_D]$ where v_0 and v are the frequency points at the line centre and at any point in the line and Δv_D is the standard frequency interval, such as the Doppler width], and $V(r)$ is the velocity of the gas at r in units of the mean thermal units (mtu). Here, $K_L(r)$ is the line-centre absorption coefficient and β is the ratio of the continuum to the line opacities. $\phi(x)$ is a profile function subjected to normalization. Further, $K_{\text{dust}}(r)$ is the absorption coefficient of dust whose source function, $S_{\text{dust}}(r, \pm\mu, x)$, is given by

$$\begin{aligned} S_{\text{dust}}(r, \pm\mu, x) & = (1 - \omega)B_{\text{dust}} \\ & + \frac{\omega}{2} \int_{-\infty}^{+\infty} P(\mu, \mu', r)I(r, \mu', x)d\mu', \end{aligned} \tag{3}$$

where B_{dust} is the Planck function for the dust emission, ω the albedo of the dust and P the scattering phase function. It is assumed that isotropic and coherent scattering hold. The quantity B_{dust} is normally neglected because the re-emission is far away from the line centre, and, therefore, may not contribute to the line radiation. Although we need not consider the term containing B_{dust} , we have included it for the sake of completeness. For other details, see Paper II and for the derivations of equations (1) and (2), refer to Peraiah, Varghese, and Rao (1987).

Finally, we calculate the total source function, S , by adding the source function, S_r , due to the reflected radiation and, S_s , due to the self radiation,

$$S = S_s + S_r. \tag{4}$$

With the above source functions and using the formal solution of the transfer equation, we calculate the line profiles along the line of sight observed at infinity.

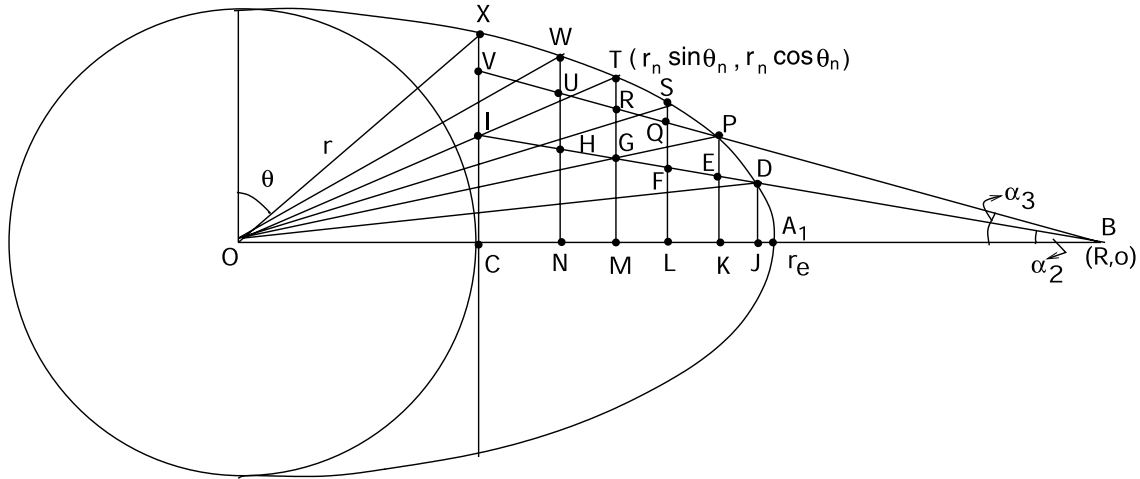


Fig. 1. Schematic diagram of the distorted atmosphere of the component.

3. Brief Description of the Parameters

We considered the atmosphere of a primary whose radius is twice as large as that of the primary with an inner radius equal to 5×10^{11} cm and an outer radius set to 10^{12} cm. The distortion is considered from the outer radius (10^{12} cm) of the atmosphere. The following are parameters used in calculation:

T_* = effective temperature of the primary component set to 2×10^4 K,

T_c = effective temperature of the secondary (with center at B, figure 1) set to 4×10^4 K,

R_{imp} = distances defined along the axis A_1O , JO , KO , ... (figure 1),

$\tau = \tau_1$ = optical depth measured along the rays, such as A_1JKL , ... , $DEFG$ (figure 1),

τ_d = dust optical depth due to dust scattering,

$v_a = 0$ is the velocity at the surface of the primary with radius $r = a (= 5 \times 10^{11})$ cm,

$v_b = 10$ mtu (mean thermal units defined in Paper I) is the velocity at the surface of the extended atmospheres with radius $r = b (= 10^{12})$ cm.

Using the above data, we compute the source functions S_r , described in Paper III, along the rays $BA_1JK \dots$, $BDEFG \dots$, $BPQR \dots$, (figure 1) and along with the axis $R_{imp} = A_1O$, JO , KO , ...

The source function, S_s , representing the self-radiation is calculated by solving transfer equations (1) and (2). We employed a complete redistribution in the line formed in a purely scattering medium ($\epsilon = 0$, where ϵ is the probability per scattering that a photon is thermalised by collisional de-excitation). The initial condition at $\tau = \tau_1$ is given in terms of the frequency-integrated Planck function ($\sigma T_*^4/4\pi$), where T_* is the effective temperature of the primary.

We considered the velocity and density law, which obeys the law of conservation of mass, namely $\dot{M} = 4\pi r^2 \rho v$, where \dot{M} is the mass-loss rate, ρ is the density, and v is the velocity

at radius r . We have considered a value of 10^{14} cm^{-3} for the electron number density at the inner radius for the purpose of calculating the optical depth. For theoretical computations, one can make different cases with all possible combinations of parameters, which obey the law of conservation of mass. The number of cases becomes more, and we obtain a huge amount of output in the form of line profiles. Thus, finally, we present one of the cases for a comparison of the source functions and line profiles with dust-free and dusty atmosphere in the following case: $v \sim r$, $\rho \sim r^{-3}$, which satisfies the conservation of mass law. We considered $\tau_d = 0$ and 5 and $r_e/R = 0.1$ and 0.5 .

4. Result and discussion

Using the above parameters, we computed the source functions for 24 rays. In practice, we can take more rays into consideration for obtaining the desired accuracy. The figures are given for $r_e/R = 0.1, 0.5$ for dusty ($\tau_d = 5$) and dust-free ($\tau_d = 0$) atmospheres, respectively. Figure 2a shows the source functions along rays (refer figure 1) A_1O , DI , PV , ... , labeled as 1, 2, 3, ... , versus the optical depths along rays 1, 2, 3, ... , respectively, for the parameters shown in the figures. The curve labeled 1 represents the source function corresponding to ray A_1O , which is the longest, because it is along the axis A_1O ($\cos \alpha = 1$). The curve labeled 24 corresponds to the source function of the rays with $\alpha = \alpha_{max}$ or with the minimum value of $\cos \alpha$ ($0 < \alpha < \pi/2$). We measured the optical depths from the points of incidence of the rays, such as A_1 , D , P , At these points, the source function is maximum for each ray and slowly falls as the optical depth increases along the rays towards the interior of the distorted medium of the atmosphere. This happens because of the fact that the incident radiation is weakened by the cosine factor. The same trend is seen in figure 4a for more radiation when we changed $r_e/R = 0.1$ to 0.5 .

Figure 2b contains the corresponding source functions (S_s, S_r, S) with respect to R_{imp} . Here, we can see three distinct curves: (i) S_s , the source function due to self-radiation,

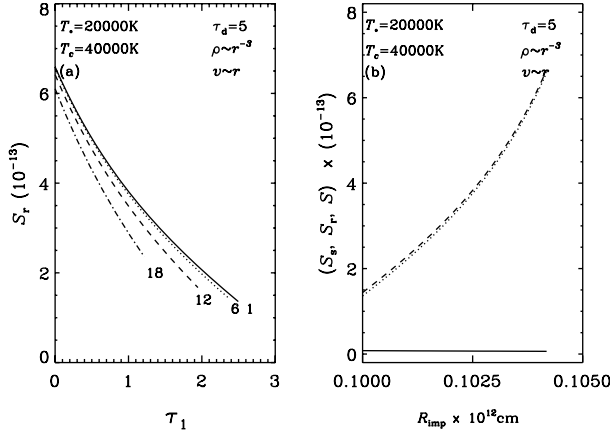


Fig. 2. Ray source function versus the optical depths along the rays for $r_c/R=0.1$ with $\tau_d=5$. In figure 2a, the continuous line for ray 1, the dotted line for ray 6, the dashed line for ray 12 and the dashed-dotted line for ray 18 are given. Figure 2b shows source functions S_s , S_r , S versus R_{imp} plotted for $r_c/R = 0.1$.

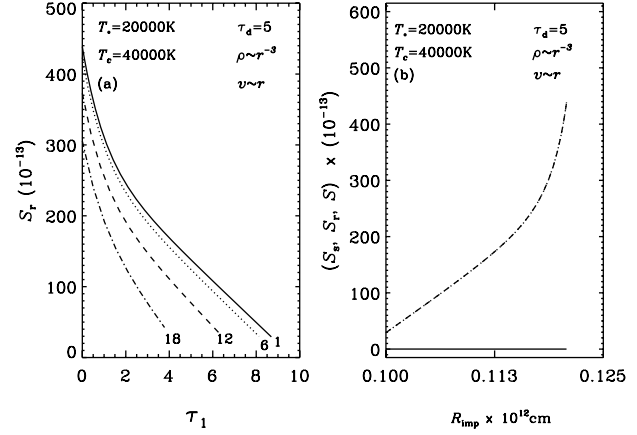


Fig. 4. Same as figure 2, but with $r_c/R = 0.5$.

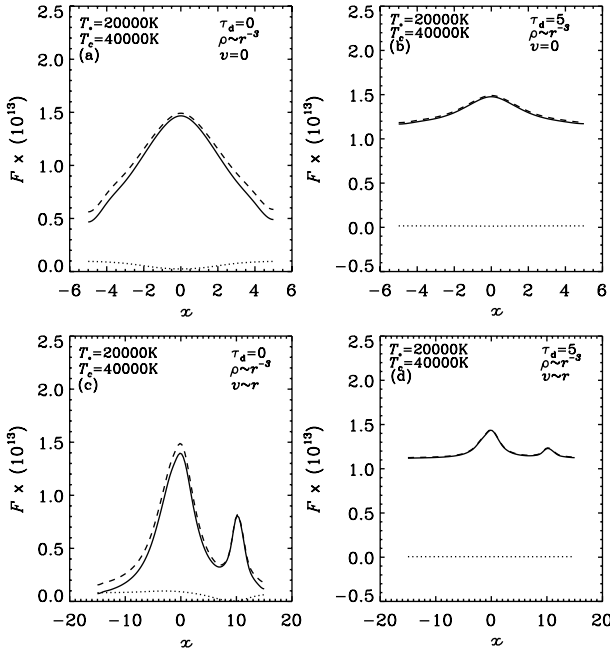


Fig. 3. Flux profiles plotted against the frequency measured in units of Doppler width x for $\rho \sim r^{-3}$. Figures 3a,b are for static media $v_a=0$ and $v_b=0$ mtu, and figures 3c, d are for the expansion velocities $v_a=10$ and $v_b=10$ mtu (mean thermal units).

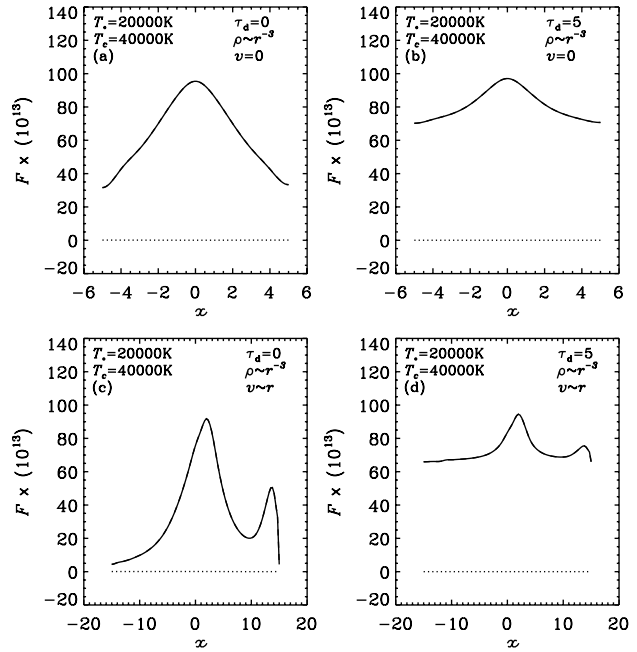


Fig. 5. Same as figure 3, but with $r_c/R = 0.5$.

represented by the continuous line; (ii) S_r , the source function of the distorted atmosphere due to irradiation, represented by the dotted line; and (iii) S , the total source function shown by the dashed line. In figure 2b and figure 4b we are not able to distinguish between S and S_r ; even the parameter r_c/R is increased from 0.1 to 0.5, which produces an increased distorted atmosphere, which can be seen in figure 4b. This is happening because the self-radiation S_s is very small and the density varies as $\rho \sim r^{-3}$ in the atmosphere.

Figures 3a, b and figures 3c, d contain the corresponding line profiles along the line of sight against frequency x for

stationary and moving atmospheres, respectively. The profiles shown by the continuous lines are due to self-radiation, S_s , while the profiles shown by the dotted line are due to the incident radiation, S_r ; the dashed lines represent the profile due to the combined source function, $S = S_s + S_r$.

Figures 3a, c and figures 3b, d also show flux profiles in dust-free and dusty atmospheres. It is interesting to note that in figures 3a, b the profile is due to self radiation, S_s , is an emission profile. Figure 3a shows that the line profile due to the incident radiation, S_r , is an absorption line without dust ($\tau_d = 0$). In the presence of dust, figure 3b, a line profile due to

irradiation, S_r , does not exist; this is because the dust scatters more photons to the wings, or more photons are removed from the core by the dust, and the dust absorbs irradiation which is incident on the surface of the primary component. We can also see that the emission peaks in figure 3a and figure 3c for static and expanding dust-free media. In the presence of dust, the emission peaks are drastically reduced in figure 3b and figure 3d, respectively, for the above reason. Another interesting point that one can bring out is that the line profiles have similar widths in figures 3a, b, c, d. In the presence of dust we obtain broad wings, as in figures 3b, d, and also dust removes the emission peaks when we compare figures 3a, c and figures 3b, d. We also notice that in the presence of the expansion velocity in figure 3c and figure 3d we obtain double-peak emission lines in dusty and dust-free atmospheres. In the presence of dust, the emission peaks are considerably reduced. Similar features are noticed in figure 5 when r_e/R increases from 0.1 to 0.5 with $\tau_d = 0, 5$.

We can thus say that profiles with a self S_s and total S radia-

tion are prominent emission lines with P Cygni characteristics. There is a perceptible change in the line profiles when the parameter r_e/R increased from 0.1 to 0.5 with $\tau_d = 0, 5$.

5. Conclusions

We have studied the effects of dust in distorted, irradiated and expanding atmospheres in the presence of gas and dust. We have considered dust-scattering optical depths as high as 5, but no absorption due to dust was included. It is found that the emission features produced due to self-radiation remain, since the irradiation effect is small. We can also note that due to dust the emission peaks are considerably reduced and the wings are broadened. Furthermore, we would like to calculate the effects of irradiation from an extended surface instead of a point source.

The author would like to thank an anonymous referee for valuable comments that improved the manuscript significantly.

References

- Ferraro, F. R., Sabbi, E., Gratton, R., Possenti, A., D'Amico, N., Bragaglia, A., & Camilo, F. 2003, *ApJ*, 584, L13
 Giuricin, G., Mardirossian, F., & Mezzetti, M. 1984, *A&A*, 131, 152
 Peraiah, A. 1969, *A&A*, 3, 163
 Peraiah, A. 1970, *A&A*, 7, 473
 Peraiah, A., & Srinivasa Rao, M. 1998, *A&AS*, 132, 45 (Paper I)
 Peraiah, A., & Srinivasa Rao, M. 2002, *A&A*, 389, 945 (Paper III)
 Peraiah, A., Varghese, B. A., & Rao, M. S. 1987, *A&AS*, 69, 345
 Peraiah, A., & Wehrse, R. 1978, *A&A*, 70, 213
 Ritter, H., Zhang, Z.-Y., & Kolb, U. 2000, *A&A*, 360, 969
 Sobolev, V. V. 1963, *A Treatise on Radiative Transfer* (New York: Van Nostrand)
 Srinivasa Rao, M., & Peraiah, A. 2000, *A&AS*, 145, 525 (Paper II)
 Stothers, R. 1974, *ApJ*, 194, 651
 Stothers, R. 1979, *ApJ*, 229, 1023
 Wehrse, R., & Kalkofen, W. 1985, *A&A*, 147, 71

